

The Influence of the Sampling Frequency of a Video Recording on a Heart-rate Detection Algorithm

Marina A. Cidota¹, Dragos Datcu² and Leon J. M. Rothkrantz³

¹*Faculty of Mathematics and Computer Science, University of Bucharest, Academiei Street No. 14, Bucharest, Romania*

²*Faculty of Technology, Policy and Management, Delft University of Technology, 2628BX Delft, The Netherlands*

³*Netherlands Defense Academy, Den Helder, The Netherlands*

Keywords: Heart-rate Detection, High Speed Camera, Frequency Sampling, Contact-free Technology.

Abstract: Contact-free technology has a great potential in different medical areas such as personal health monitoring and telemedicine. One of the physiological parameters that can be measured with this type of technology is the heart rate. The pulse is proportional with the physical effort or mental stress, its measurement being an important issue in sport, medicine and psychology. In this paper we present an analysis of the accuracy of the heart rate detection using a high speed camera for recording a color video with the face of a person. The recordings were done both from frontal view and from profile and they were resampled to different frequencies between 10 and 240 frames per second. From our tests we may conclude that it was not the high frequency but the quality of the videos recorded with a high speed camera that allowed us to reduce the time needed to obtain the heart-rate up to 5 seconds. We have also noticed that the results are influenced by the errors generated in the resampling process of the video signal.

1 INTRODUCTION

The idea of a non-contact device for determining different physiological measurements was first implemented in 1997 by Greneker (Greneker, 1997) who used the radar technology to measure from distance (up to 10 meters) the pulse and respiration rate of a person. In 2007, Garbey (Garbey et al., 2007) used a thermal camera that recorded the temperature fluctuation of the carotid region and based on FFT of this signal they computed the heart rate with a very high accuracy. In 2010, Poh (Poh et al., 2010) proposed an ICA (independent component analysis) based algorithm for detecting the heart rate from a color video recording of a face done with a web camera. They applied an optical technique called photoplethysmography (PPG) that can be used to detect blood volume changes in the microvascular bed of tissue from a selected skin area (Allen, 2007). The PPG waveform is attributed to cardiac synchronous changes in the blood volume with each heart beat. Although the origins of the components of the PPG signal are not fully understood, it is generally accepted that they can provide valuable information about the cardiovascular system. The PPG technology has been successfully used in a wide range of commercial medical

devices for measuring oxygen saturation, blood pressure, heart rate, respiratory rate and also detecting peripheral vascular disease.

During the cardiac cycle, the superficial blood vessels from face change their volume and this can be found in the variation of the amount of reflected light. By recording a color video of the facial region, the ICA (Cardoso and Souloumiac, 1993; Comon, 1994) can be applied to the RGB components to separate the plethysmographic signal from other sources of fluctuations in light due to artifacts. Once the plethysmographic signal is identified, a spectral analysis is used to compute the heart-rate value. Having a video recording of a face from a web cam, to obtain an accurate response the window used for computing the heart rate has a length of 30 seconds (Poh et al., 2010). One of the restrictions of the existing methodology is that the person remains as still as possible during the recording of the video.

In our work, we used a high speed camera with the goal of analyzing the influence of the frequency sampling of the video recordings over the heart-rate value computed from the RGB signals. The recordings were done both from frontal view and from profile and they were resampled to different frequencies between 10 and 240 frames per second. Taking ad-

vantage of the quality of the videos recorded with the camera that we used, we managed to reduce the length of the time window needed to compute the heart-rate up to 5 seconds, as we describe below. We have also noticed that it is not high sampling frequency of the video signal but having a small resampling error that leads to more accurate results.

2 METHODS

2.1 Recordings

With the Pike high speed camera from Allied Vision Technologies, we have done color video recordings with six white persons with different complexions, out of which one wearing glasses and another having a beard. The recordings were done both from frontal view and from profile, with the sunlight as the only source of illumination, and we asked the subjects to remain as still as possible for 30 seconds. For only one person we did two sets of recordings, before and after making physical effort (climbing stairs).

The frequency of the camera cannot be set directly, it depends on other parameters (like shutter, gain, whitebalance, gamma etc.) and also on the dimension of the frames. With a set of values that we chose (shutter=100, gain=444, whitebalance=357, gamma=1 and pixel resolution of 252×350), we computed the ratio between the time length and the number of frames of a video recording and we got a frequency of 241.9 frames per second (fps). We re-sampled each video to different frequencies between 10 and 240 fps.

To be able to see the performance of the algorithm for heart-rate detection, we needed a device to provide us accurate measurements of the pulse. We used the Mobi 8 device produced by TMS International B.V. which is able to measure the pulse at 2048 Hz.

In order to reduce the computational complexity of our software implementation, for each video recording we set a fixed rectangular region of interest (ROI) as shown in Figure 1. From each frame of a video we retained three elements representing the mean values of RGB extracted from the ROI, so for each video, with a frequency sampling F_s , the input data for the heart-rate algorithm is a matrix with $30 \times F_s$ rows and 3 columns. For the software implementation of this part we used the C++ programming language with the OpenCV library. The heart-rate detection algorithm was written in MATLAB and we used the JADE (Joint Approximate Diagonalization of Eigen-matrices) MATLAB implementation for ICA (Cardoso and Souloumiac, 1993).

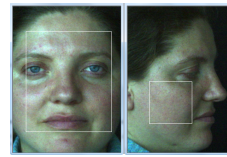


Figure 1: (a) Frontal view ROI; (b) Profile ROI.

2.2 Algorithm for Detecting Heart-rate

The main ideas for the heart-rate algorithm were taken both from (Garbey et al., 2007) and (Poh et al., 2010; Poh et al., 2011). As shown in Figure 2, at each step of the algorithm we compute a heart-rate value from a 5 second window extracted from the RGB signals and, for the next step of the algorithm, we move the window with one second to the right and so on until we reach the end of the signal.

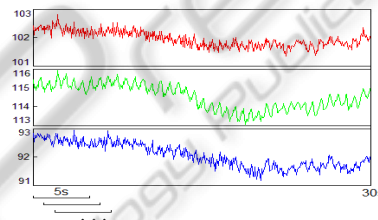


Figure 2: The RGB components obtained by averaging the red, green, respectively blue values of the pixels from the ROI.

We now describe the computations that we do within the 5 second-length window in order to obtain a heart-rate value. Regarding the length of the window, our goal was to use the shortest possible length for which the heart-rate detection algorithm provides good results. From many tests we have done with different lengths between 3 and 10 seconds, we came to the conclusion that a 5 second-length window is the optimal choice.

Before applying ICA to the three RGB signals, we filter them to keep only the stationary components. Time and frequency domain methods have been usually applied to heart rate variability (HRV) analysis. Spectral density estimation inherently assumes that the signal is at least weakly stationary. Thus, the non-stationarities in the HRV signal can cause distortion to frequency domain analysis and to get over this problem we applied the detrending method presented in (Tarvainen et al., 2002). Each RGB signal may be decomposed in two parts

$$x = x_{stat} + x_{trend} \quad (1)$$

where x_{stat} is the nearly stationary component and x_{trend} is the low frequency trend component which can be removed using a detrending method that behaves

like a time-varying high-pass filter. The frequency response of the filter depends on a parameter λ , and this dependence is presented in Figure 3 (Tarvainen et al., 2002). The cut-off normalized frequency of the filter decreases when λ is increased.

The values for λ were chosen so that the detrending procedure would not affect the range of frequencies that we are interested in, which is between $[0.7, 4]$ Hz (corresponding to the heart-rate values between $[42, 240]$ beats per minute (BPM)). For instance, if $F_s = 15$ and $\lambda = 10$ then the cut-off frequency is $0.059 * 15 \approx 0.89$ Hz. In setting the other values for λ we guided after the graphs plotted in Figure 3 and we displayed these values together with the resampling frequencies F_s in Table 1.

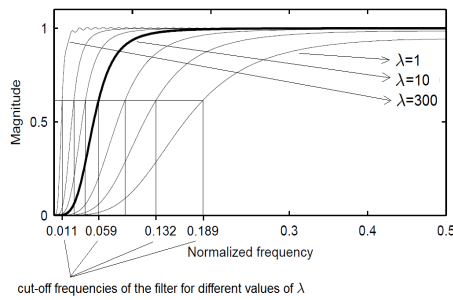


Figure 3: Frequency responses of the detrending filter for $\lambda = 1, 2, 4, 10, 20, 50$ and 300 . The corresponding cut-off frequencies are $0.189, 0.132, 0.093, 0.059, 0.041, 0.025$ and 0.011 times the sampling frequency.

Table 1: Values for the parameter λ used in the detrending algorithm.

F_s	15	25	30	45	60
λ	10	25	30	70	90
F_s	75	100	120	200	240
λ	200	330	400	700	800

A requirement for applying ICA is that the signals are normalized, so the detrended signals $x_1(t)$, $x_2(t)$ and $x_3(t)$ become

$$y_i(t) = \frac{x_i(t) - \mu_i}{\sigma_i}, i = 1, 2, 3,$$

where μ_i and σ_i are the estimated mean and standard deviation of $x_i(t)$.

Although the order in which the ICA separates the independent component is unknown, for all the video recordings we tested it was always the second component which contained the heart-rate signal.

To increase the robustness of the algorithm to transient noise that may appear during recordings, we divide the 5 second window in two parts. The last 4 seconds from each window were used to compute the

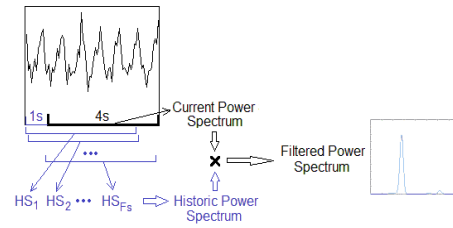


Figure 4: A 5 second window from the second component returned by ICA.

current power spectrum P . The first second of the signal contains F_s points. A power spectrum is computed from a 4 second window starting from each point, and thus we obtain a number of F_s spectra denoted by HS_1, \dots, HS_{F_s} (see Figure 4). The historic power spectrum is then defined as

$$H(f) = \frac{\sum_{i=1}^{F_s} HS_i(f)}{\sum_{f=1}^{F_s} \sum_{i=1}^{F_s} HS_i(f)}, \quad (2)$$

where L is the number of points where FFT is computed for each 4 second length window. The filtered power spectrum F is computed as the pointwise product between the current power spectrum P and the historic power spectrum H (see Figure 5)

$$F(f) = P(f) \times H(f), f = 1, \dots, L. \quad (3)$$

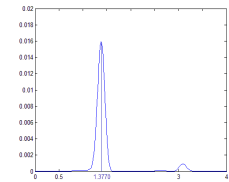


Figure 5: Filtered power spectrum computed from a 5 second window.

For the frequency range that we are interested in, which is $[0.7, 4]$ Hz, we determine the frequency with the maximum energy from the filtered power spectrum, then we multiply it by 60 to get the heart-rate value. For the case shown in Figure 5, the heart-rate value would be $1.3770 * 60 = 82.62$, i.e. 83 BPM.

In order to remove the influence of accidental noise on the heart-rate signal, besides the application of ICA and using the historic power spectrum, we set a threshold of 12 BMP to control the difference between two successive heart-rate values computed from the frequency with the maximum energy. If the difference exceeds the threshold, we keep the previous heart-rate value instead of the current one.

3 RESULTS

Simultaneously with the video recordings we also measured the pulse of each person. From the data provided by the Mobi 8 device, we retained only the pulse values measured at one second distance from one another. Thus, for each 30 second video recording we had the corresponding 30 element vector with the heart-rate values. Each video is analyzed with the 5 second window that is shifted with one second at every step of the algorithm. So, from a 30 second recording we obtain 26 values that we interpret as being the heart-rate. To be able to make a comparison between these values and the ones that represent the ground truth measurements, we computed moving averages of order 5 from the heart-rate values given by the Mobi 8 device (see Figure 6).

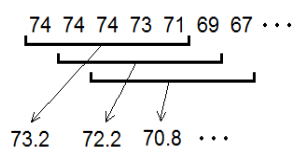


Figure 6: Moving averages of order 5 from the heart-rate values.

The recordings, both from frontal view and from profile, were resampled to different frequencies between 10 and 240 frames per second. Since the range of frequencies that we are interested in is $[0.7, 4]$ Hz, we considered as the lowest frequency for analysis a value ($F_s = 10$) that is greater than twice the upper limit of the frequency interval (the Nyquist theorem).

Regarding the resampling process, we have performed it in two ways. First, we selected the frames with a constant integer step computed as the integer part of the ratio between the recording frequency and the new frequency used for resampling ($step = integer(241.9/new_fs)$). The resampling errors depend on the fractional part of the ratio $241.9/new_fs$ and these errors proved to have a great impact over the performance of the heart-rate detection algorithm. For instance, the error for resampling to $new_fs = 15$ is small ($241.9/15 = 16.1267$) in comparison with the error associated with $new_fs = 25$ ($241.9/25 = 9.6760$) and the differences in performance can be observed in Figure 7. The results shown are obtained from the same video resampled with a constant step using different frequencies (small resampling errors on the left side, big resampling errors on the right side in Figure 7). The sampling frequencies are shown in the right lower corner of each graphic. The dotted lines represent the ground truth values of the heart-rate and the continuous line is given by the output of the algorithm. In the upper part we also plotted two

values: the left one is the average of the heart-rate values computed by the algorithm and the right one is the average of the real values of the heart-rate.

The second approach for the resampling process consists of computing the exact position and choosing the closest frame in the source video (nearest neighbor approach). That implies that for each resampling performed, the frames are selected with a variable step. Using this technique, we have resampled each video recording to the frequencies 10, 12, 15, 25, 37 and 203 fps (some of these values were chosen randomly). For the frontal view ROI we have obtained very good results for each mentioned frequency (see Figure 8). With few exceptions, from all the other frontal view recordings we obtained results that are very similar to those presented in Figure 7 and in Figure 8.

Regarding the video recordings with the profile ROI, we also obtained good results but the resampling frequencies proved to have a greater influence over the performance of the heart-rate detection algorithm. A possible explanation for this could be the fact that the area of the profile ROI is smaller and thus it is much more sensitive to noise than the frontal view ROI. Besides the resampling errors, each video recording is affected by a pseudo-random noise which introduces big/small distortions at different sampling frequencies. The noise may come from the camera, from small movements that a person makes during a recording and from variation of the sun light.

In Table 2 we display the results computed from the recordings with the profile ROI resampled to 15 fps (with constant step) and 25 fps (using the nearest neighbor approach). Compared to the other frequencies used, these are the best results we obtained with respect to the two types of resampling methods that we applied.

Table 2: The results obtained for the recordings with the profile ROI resampled to 15 fps and 25 fps.

recording no.	real mean value of the heart rate	mean value at 15 fps	mean value at 25 fps
1	73.9615	71.5633	79.9467
2	56.8462	54.4584	54.5373
3	69.8154	68.8251	69.5519
4	76.5462	74.5380	76.0310
5	76.6308	75.2479	76.0874
6	71.2846	70.3463	72.1717
7	93.1000	91.6091	92.0035

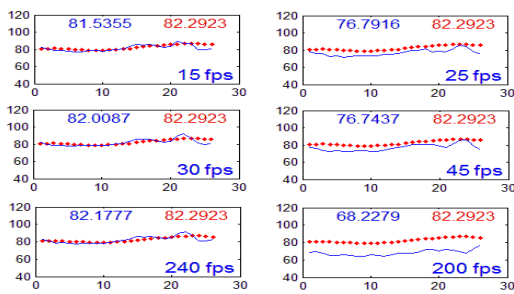


Figure 7: Results obtained from one recording resampled to different frequencies. The dotted lines represent the ground truth values of the heart-rate (the average value is plotted on the right); the continuous line is given by the output of the algorithm (the average value is plotted on the left).

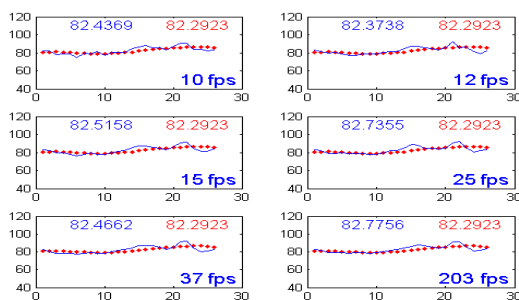


Figure 8: Results obtained from the same recording as in Figure 7 resampled to different frequencies using the nearest neighbor approach.

4 CONCLUSIONS

In this paper we presented the results obtained by a spectral analysis algorithm for heart-rate detection from color video recordings of the face of a person (both frontal view and profile).

From different tests made with our recordings, we have noticed that the sampling frequency used for video may affect the accuracy of the results. This influence is due both to the resampling errors and to the noise that introduces different distortions when it is sampled to different frequencies. In most cases, when the resampling error was small, the frontal view ROI gave very good results. In contrast, a high resampling error usually led to results that were less than the real heart-rate values. The profile ROI that we considered in our experiments proved to be more sensitive to the choice of the sampling frequency, but nevertheless, as we could see in Table 2, proper values of the frequency also provide good results.

From all the experiments we have done, we may conclude that using a high sampling frequency for the video recordings does not lead to a higher accuracy of the results in our specific problem. The main ad-

vantage of the high speed camera over a simple web cam does not lie in the possibility of recording more frames per second, but in achieving a better quality of the video, which allowed us to reduce the time length of the window we used to compute a heart-rate value to 5 seconds. Taking into account the computational complexity, we consider that $F_s = 25$ fps is the highest frequency that should be used for the video recordings with the Pike camera.

As a future work related to the topic presented in this paper, we intend to make new video recordings with the Pike camera using artificial light as source of illumination to see if it interferes and affects the heart-rate signal extracted from ROIs with different sizes and positions on the face.

ACKNOWLEDGEMENTS

This work was supported by the strategic grant POSDRU/89/1.5/S/58852, Project "Postdoctoral programme for training scientific researchers" cofinanced by the European Social Fund within the Sectorial Operational Program Human Resources Development 2007-2013.

REFERENCES

- Allen, J. (2007). Photoplethysmography and its application in clinical physiological measurement. In *Physiological Measurement*, vol. 28, pp. R1-R39.
- Cardoso, J.-F. and Souloumiac, A. (1993). Blind beamforming for non gaussian signals. In *IEE Proceedings-F*, vol. 140, no. 6, 362–370.
- Comon, P. (1994). Independent component analysis, a new concept? In *Signal Processing*, 36, 287-314.
- Garbey, M., Sun, N., Merla, A., and Pavlidis, I. (2007). Contact-free measurement of cardiac pulse based on the analysis of thermal imagery. In *IEEE Trans. Biomed. Eng.*, vol. 54, no. 8, 1418–1426.
- Greneker, E. (1997). Radar sensing of heartbeat and respiration at a distance with application of the technology. In *RADAR*, vol. 97, no 449, 150–154.
- Poh, M., McDuff, D., and Picard, R. (2010). Non-contact, automated cardiac pulse measurements using video imaging and blind source separation. In *OPTICS EXPRESS*, Vol. 18, No. 10.
- Poh, M., McDuff, D., and Picard, R. (2011). Advancements in noncontact, multiparameter physiological measurements using a webcam. In *IEEE TRANSACTIONS ON BIOMEDICAL ENGINEERING*, VOL. 58, NO. 1.
- Tarvainen, M., Ranta-Aho, P., and Karjalainen, P. (2002). An advanced detrending method with application to hrv analysis. In *IEEE Trans. Biomed. Eng.*, vol. 49, no. 2, 172–175.